Published in final edited form as:
J Am Chem Soc. 2013 September 11; 135(36): . doi:10.1021/ja4075997.

Stress-Responsive Polymers Containing Cyclobutane Core Mechanophores: Reactivity and Mechanistic Insights

Zachary S. Kean[†], **Zhenbin Niu**[†], **Gihan B. Hewage**[†], **Arnold L. Rheingold**[‡], and **Stephen L. Craig**[†,*]

[†]Department of Chemistry, Duke University, Durham, North Carolina 27708, United States

[‡]Department of Chemistry, University of California, San Diego, La Jolla, California 92093, United States

Abstract

A primary goal of covalent mechanochemistry is to develop polymer bound mechanophores that undergo constructive transformations in response to otherwise destructive forces. The [2+2] cycloreversion of cyclobutane mechanophores has emerged as a versatile framework to develop a wide range of stress-activated functionality. Herein, we report the development of a class of cyclobutane bearing bicyclo[4.2.0]octane mechanophores. Using carbodiimide polyesterification, these stress-responsive units were incorporated into high molecular weight polymers containing up to 700 mechanophores per polymer chain. Under exposure to the otherwise destructive elongational forces of pulsed ultrasound, these mechanophores unravel by ~7 Å per monomer unit to form □,□-unsaturated esters that react constructively via thiol-ene conjugate addition to form sulfide functionalized copolymers and cross-linked polymer networks. To probe the dynamics of the mechanochemical ring opening, a series of bicyclo[4.2.0]octane derivatives that varied in stereochemistry, substitution, and symmetry were synthesized and activated. Reactivity and product stereochemistry was analyzed by ^{1}H NMR, which allowed us to interrogate the mechanism of the mechanochemical [2+2] cycloreversion. These results support that the ring opening is not concerted, but proceeds via a 1,4 diradical intermediate. The bicyclo[4.2.0]octanes hold promise as active functional groups in new classes of stress-responsive polymeric materials.

Covalent mechanochemistry has enabled the development of a wide array of stress-responsive polymers for application in the fields of catalysis,[1–3] synthesis,[4] stress-sensing,[5–7] and self-healing or self-strengthening materials[8] among others. Generally, these mechanochemical transformations are facilitated by polymeric handles, which act as force transducers to direct applied stress to the mechanophore of interest from bulk stress or shear flow,[9] but the relationship between macromolecular and intermolecular forces[10] has allowed molecular force probes to be used to productive effect as well.[11–13] Many of the reported mechanochemical transformations are inherently dissociative,[14–18] leading to the chain rupture and molecular weight degradation as a result of their activation. Non-scissile mechanophores allow for several unique molecular responses in the context of stress responsive material systems. First, because non-scissile activation events occur independently of molecular weight degradation, many reactive functionalities may be generated per chain rupture event (i.e. non-specific chain scission in pulsed ultrasound),

*Corresponding Author: stephen.craig@duke.edu.

The authors declare no competing financial interest.

Supporting Information. Experimental details, synthetic procedures, GPC characterization, sonochemical methods, structure determination, crystallographic data, and additional details. This material is available free of charge via the Internet at http://pubs.acs.org.

giving the opportunity for constructive bond formation to outpace destructive bond scission in materials under load.[19,20] Second, high local elongations[21,22] can be engineered into these mechanophores, and may provide a basis for molecular level stress-relief in overstressed subchains in bulk materials under load. These aspects of mechanophore design are heavily influenced by our goal of developing an "on-demand" response in materials under destructive stress in order to delay or prevent catastrophic failure.

Previously, we have explored the *gem*-dihalocyclopropanated (*g*DHC) polybutadiene platform to this end. The *g*DHC mechanophores elongate by ~1.5 Å per cyclopropane and generate reactive 1,3-diradicals or 2,3-dihaloalkenes upon activation.[23] Recently, we utilized this platform to demonstrate a liquid-to-solid transition in polymer solutions under destructive shear as well as stress-induced bond formation and crosslinking in the bulk.[8] Other reported non-scissile mechanophores include benzocyclobutenes,[24] atropisomeric biaryls,[25] epoxides,[26] spiropyrans,[27] pyrophosphates,[28] and oxanorbornadiene.[29] The Moore group has demonstrated that cyclobutane bearing acrylate polymers exhibit enhanced scission kinetics under the application of pulsed ultrasound leading to the production of functional chain-end acrylates in a net [2+2]cycloreversion.[30,31] We sought to utilize this tranformation to develop a new class of non-scissile mechanophores based on fused-cyclobutane structures via the installation of a covalent tether. Previous efforts have demonstrated a photoreversible, single mechanophore system embedded in poly(methyl acrylate).[32] Here, we expand the non-scissile mechanophore repertoire by incorporating bicyclo[4.2.0]octane (BCO) functionality into high molecular weight (MW) polyesters via carbodiimide polyesterification[33] of BCO containing diester diols. We also use the BCO platform to analyze stereochemical effects on mechanochemical reactivity, for potential self-healing applications via stress-generated □,□-unsaturated ester functional groups, and as a tool for mechanistic inquiry through analysis of stereochemical product distributions.

Results and Discussion

Initially, we aimed to develop a modular and scalable (multi-gram) approach to synthesize fused-cyclobutane bearing monomers. As previously reported,[34] *cis*-BCO dicarboxylic acid **1a** (Scheme 1) can be prepared in large quantities (~10 g, see Supporting Information) by photochemical [2+2] cycloaddtion of maleic anhydride and cyclohexene in the presence of benzophenone. Basic hydrolysis of the anhydride followed by acidification allows for the precipitation of the carboxylic acid from water in high diastereomeric purity (95%,^{1}H NMR, see Supporting Information). Acid-catalyzed esterification with ethylene glycol yields diol-functional *cis*-BCO **1**. Carbodiimide polyesterification, based on the method of Moore and Stupp,[33] of the diol monomer in the presence of glutaric acid, diisopropylcarbodiimide, and DPTS (dimethyl-aminopyridinium *p*-toluenesulfonate) in DCM (Scheme 2A) yields high-molecular weight polyester (179 kDa, Table 1). High MWs are routinely attainable with this method when polymerization is performed for 48 hours at high monomer concentration (~0.5–1 M). Polymers were characterized by gel permeation chromatography-multi-angle light scattering (GPC-MALS), and undergo multiple chain breaks per polymer chain (on average) during sonication experiments.

Mechanochemical activity was probed via the application of pulsed ultrasound (14.8 W/cm^2, 6–9 °C) to **P1** (*cis*-BCO)(179 kDa, MeCN, 2 mg/mL). Subsequent ^{1}H and ^{13}C NMR analysis revealed the presence of peaks consistent with □,□-unsaturated ester formation, the first direct spectroscopic observation of alkenes formed via the mechanochemical [2+2] cycloreversion of cyclobutanes (Figure 1, see Supporting Information). These resonances were observed to increase as a function of sonication time, reaching 48% ring opening after 180 minutes of sonication time, corresponding to the production of 450 alkenes per initial polymer chain. Due to the non-scissile nature of the mechanophore, many alkenes are

formed per chain scission event, allowing for the quantification of percent ring opening (vs. initial BCO content, see Supporting Information) at various sonication times with concurrent MW degradation via non-specific chain scission due to the high forces commonly generated during ultrasonication. Using established molecular modeling methods[21,35] (see Supporting information), we estimate that elongations of ~7 Å per polymer repeat unit occur as the *cis*-BCO mechanophore unravels under applied stress. This magnitude of covalent stress relief per event exceeds that reported previously,[5,22,32] and might permit survival of overstressed polymer subchains under strains that are otherwise catastrophic.[23]

To demonstrate the mechanochemical nature of the ring opening, we synthesized control polymer **PC** (13.3 kDa, Table 1). Flow forces experienced by low MW polymers are often insufficient to illicit many covalent mechanochemical transformations by pulsed ultrasound, while activation due to purely thermal processes presumably remains unaffected.[9] After 180 minutes of irradiation, polymer **PC** showed no ring opening or appreciable MW degradation (see Supporting Information).

With the ability to quantify the extent of the mechanochemical [2+2]cycloreversion, we decided to use our platform to probe the relative reactivity of *cis* and *trans* handles to applied force. Previous observations have shown that mechanophores with *trans* attachment points display diminished activation kinetics when compared to their *cis* counterparts.[24,30,36] In the case of benzocyclobutene, this has been attributed to a combination of lower force-free activation energy, greater chemo-mechanical coupling efficiency, and larger changes in compliance along the reaction coordinate between ground and transition states for the *cis* isomer.[37–39] The *trans*-BCO monomer **2** was obtained by base-mediated epimerization of *cis*-BCO (dimethylester) with sodium methoxide and subsequent transesterification with ethylene glycol (see Supporting Information). The *cis* and *trans* diols were copolymerized into a single polymer **P1,2** (*47:53 cis:trans*, 161 kDa, Table 1) to ensure that the average forces experienced by each isomer were identical during sonochemical experiments. As shown in Figure 2, the percent ring opening for the *cis* isomer exceeded that of the *trans* at all times tested, further validating the observations of Kryger et. al.[30] It should be noted that while the ring opening disparity diminishes throughout the sonication (from *cis:trans* 2.5:1 at 5 min to 1.6:1 at 180 minutes), this is consistent with exhaustion of the *cis* isomer in the mechanically susceptible region of the polymer chains.[15,40,41]

The unveiled □,□-unsaturated esters are reactive toward a variety of conjugate addition conditions, allowing us to expand the repertoire of stress-induced bond forming reactions. To test the potential for our polymers as self-healing materials we targeted the nucleophilic thiol-ene reaction. *Cis*-BCO polymer **P1** was first sonicated for 180 min (4 mg/mL) to yield a 33% ring-opened polymer. To characterize the efficiency of the reaction, we first reacted the polymer with a mono-functional thiol, ethyl thioglycolate (1.5 eq. per alkene) in acetonitrile-d_3 (~0.1 mmol alkene), with 1,8-diazabicyclo[5.4.0]undec-7-ene (DBU, 0.5 mol %) catalyst. Time points were recorded by ^{1}H NMR and near complete conversion of the alkenes were observed in 65 minutes. Encouraged by the efficiency of the reaction, we subjected a 36% ring-opened *cis*-BCO polymer to identical reaction conditions in the presence of difunctional 1,4-butanediol bis(thioglycolate) (0.5 eq. per alkene) yielding an intractable polymer gel in less than 1 minute (Figure 3). These results demonstrate the potential of this system to participate in an expanded array of bond forming reactions that occur rapidly under relatively mild (ambient) conditions. Current efforts focus on expanding this approach to *in situ* bond formation both in solution and in bulk materials. This involves both the construction of BCO-containing materials that encourage bulk mechanochemical activation as well as developing BCO analogues that increase the reactivity of the unveiled unsaturation to non-catalyzed conjugate addition.

While exploring the sonochemical reactivity of the *cis*-BCO systems, we were intrigued by the stereochemistry of the mechanochemically generated alkenes (Figure 1). We observed two sets of overlapping peaks in the ^{1}H NMR spectrum (H_A, ~6.95 ppm) corresponding to the □,*E*-alkene proton. We presumed that this was due to differing shifts for *EE* and *EZ* pairs within a single monomeric diene. Lorentzian deconvolution of a representative peak (180 min sonication time, see Supporting Information) revealed that the major isomer accounts for 76% of the total □,*E*-alkene proton integration. Due to the relative total *E:Z* content (51:49) and less resolution between peak overlap for the remaining resonances, we were unable to obtain the stereochemical product distribution without ambiguity via this method (although the possibilities were narrowed to two possible outcomes, see Supporting Information). Instead, the identity of the major *E*-containing isomer was confirmed by reducing the esters of sonicated *cis*-BCO with Dibalh to diol derivatives of the constituent esters, specifically deca-2,8-diene-1,10-diols from the mechanochemically generated □,□-unsaturated esters (Figure 4a). Gas chromatography (GC) analysis of the TMS-derivatized product mixture versus authentic compounds showed that the *EZ*-isomer was produced as the major product (78%), followed by the *EE* (14%) and *ZZ* (8%) isomers (Figure 4b). This corresponded well to a possible product distribution of 77:13:10 previously determined by deconvolution of the ^{1}H NMR spectrum (see Supporting Information).

The opportunity to quantify a mixture of products in a mechanochemical reaction is unique among examples to date, and here the product stereochemistry provides an opportunity to experimentally probe the mechanism of mechanochemical cyclobutane cleavage, which was previously shown computationally to proceed through a sequential bond breaking process.[31] The generation of *EZ* products from *cis*-BCO represents a formal inversion of configuration at C1 or C2, facilitated by a formal rotation about either the C1-C4 or C2-C3 bonds prior to formation of the product alkenes. Though once the subject of debate,[42–44] it is generally accepted that [2+2] cycloreversions of cyclobutanes occur through highly non-concerted two step processes via a tetramethylene diradical intermediate.[45] Experimental[46] and theoretical[47] evidence, however, suggests that some preference exists for inversions (via bond rotation in the tetramethylene intermediate) that reflect the outcomes of hypothetical $2\pi_s+2\pi_a$ orbital symmetry allowed pathways, perhaps as a result of through-bond coupling in the diradical. Additionally, mechanochemical reaction mechanisms often deviate from canonical pathways[24,48] and deserve further interrogation. The most obvious deviation from force-free behavior in the present case is that the cycloreversion occurs with different regioselectivity from the force-free thermal process for bicyclo[4.2.0]octane, which degrades to cyclohexene and ethylene[46] (as opposed to 1,7-octadiene).

We discuss the mechanism in terms of two limiting pathways: (a) inversion via a $2\pi_s+2\pi_a$ (Woodward-Hoffmann allowed) concerted [2+2]cycloreversion (Figure 5a) and (b) formation of a diradical intermediate via C1–C2 homolytic cleavage and subsequent rotation in kinetic competition with product (alkene) formation (Figure 5b). We omit from consideration $2\pi_s+2\pi_s$ thermally disallowed concerted pathways due to the exceptionally high activation energy (~115 kcal/mol) determined by Woodward and Hoffmann[49] (in that this is significantly higher than the activation energy of cyclobutane ~62 kcal/mol[50]).

Taken alone, mechanochemical activation of *cis*-BCO leaves little room to comment on which pathway is primarily at play, as the *EZ* product might result from either mechanism (Figure 6a). We therefore synthesized a *trans*-BCO homopolymer **P2** (95% *trans*, 155 kDa) in order to observe whether the product stereochemisry has a memory of the reactant stereochemistry. After 180 min of sonication and reduction, the *trans*-BCO ring opening was analyzed by the GC and ^{1}H NMR deconvolution methods performed previously for **P1** (see Supporting Information). Again, the *EZ* isomer was observed to predominate (71%), though to a slightly lesser extent when compared with *cis*-BCO (Figure 6b). The formation of the

EZ isomer from *trans*-BCO represents a formal retention of stereochemistry, versus a formal inversion from the *cis*-BCO isomer. The similar product distributions for the two isomers suggest that the two ring openings occur via a two-step process with a common intermediate (taken to be the tetramethylene diradical), followed by a stereochemistry determining step (C3–C4 homolysis, Figure 5b). In this scenario, the diradical is pulled into a preferred "*pro-EZ*" conformer prior to or concurrent with product formation (Figure 6c). We note that while most memory of the initial stereochemistry is lost, some remains; the relative product distributions for both isomers are skewed slightly toward the corresponding single inversion products (more *EZ* for *cis* and *EE/ZZ* for *trans*) predicted for 2_s+2_a cycloreversion pathways. It should also be pointed out that the diradical conformers shown in Figure 5 are meant to be convenient representations of the dynamics involved during cycloreversion and do not necessarily represent all aspects of electronic and molecular structure involved.

An alternate view of these "memory" effects is to couch them in terms of the dynamics of the diradical intermediate. Once the diradical forms (via C1–C2 homolysis), alkene formation via C3–C4 cleavage can occur either before or after conformational relaxation, for example through rotation about C1–C4 or C2–C3. Scission prior to relaxation ($k_{break} \gg k_{rot}$) corresponds to an effectively concerted (if highly asynchronous) mechanism, whereas $k_{rot} \gg k_{break}$ corresponds to the purely stepwise process. Within this framework, the *cis* vs. *trans* BCO reactivity is consistent with minor contributions from C3–C4 scission prior to conformational relaxation; in other words, $k_{rot} > k_{break}$, but there is some competition between the processes. We therefore set out to hinder the rotation by increasing sterics at C1 and/or C2.

Initially, we installed a single nitrile group on the cyclobutane ring. Purification by column chromatography yielded the asymmetrically substituted *cis*-CN-BCO dimethyl ester as the major product (single diastereomer **3a**, see Supporting Information), the structure of which was confirmed by X-ray crystallography (see Supporting Information). Transesterification with ethylene glycol yielded the diol monomer **3**, which was polymerized in the previously described fashion (Scheme 2) to yield a 133 kDa polyester **P3** (Table 1). The overall reaction stereochemistry was largely unchanged; Lorentzian deconvolution, which is sufficient to determine the product distribution unambiguously in this case, was utilized to determine the major product to be the EZ_{CN} diene (77%, Figure 7a, see Supporting Information). Little inversion was observed about the nitrile functionalized C1-C4 bond, with 98% of the cyanoalkenes obtained in the *Z*-configuration. Additionally, further support is given for the preference of a "pro-*EZ*" conformer in that the overall product ratios (*EZ:EE:ZZ*) is consistent with that of the unsubstituted *cis*-BCO and *trans*-BCO mechanophores (Figure 6c), indicating that the same preference for the formation of a "pro-*EZ*" conformer occurs even when rotation about one bond of the diradical is restricted. This outcome can be rationalized in the context of the non-concerted diradical intermediate where $k_{rot,H} > k_{rot,CN}$ but $k_{rot,H} > k_{break}$, as the initial configuration of the C2–C3 bond is lost in the majority of cases. Similar effects are observed with respect to substitution in the thermolysis of aliphatic cyclobutane derivatives.[51]

We sought to determine whether additional substitution would further disfavor the formation of the *EZ* isomer and bias the reaction outcome towards net formal retention of initial configuration. By subjecting *cis*-BCO diacid **1a** to Hell-Volhard-Zelinsky conditions as previously reported,[52,53] we were able to isolate the dimethyl ester of *cis*-Br_2-BCO (*meso*) as a single diastereomer confirmed by X-ray crystallography (see Supporting Information). Analogous to previous diols, **4** was synthesized by acid-catalyzed transesterification with ethylene glycol. Polyesterification of **4** proved more challenging than previous examples, but we obtained polymer **P4** (51 kDa, Table 1) that was sufficient for sonochemical activation and product analysis. The polymer was subjected to pulsed ultrasound (180 min)

in $CHCl_3$ (due to insolubility in MeCN), and 12% ring opening was observed by ^1H NMR. Unlike previous polymers, *Z*-alkene products predominated, accounting for 80% of all alkenes formed (note: due to a change of priority designation, the *Z*-configuration here is equivalent to the *E*-configuration of previous examples with respect to retention of stereochemistry). Again, Lorentzian deconvolution was sufficient to determine stereochemical product distributions. As hypothesized, the *ZZ* isomer was observed to be the major product (66%), corresponding to both a formal retention of stereochemistry, as well as a shift in preference away from the proposed "pro-*EZ*" conformer, in contrast with all preceding examples (Figure 7b and 7c). The differences in product distribution for **P4** are not due to its lower molecular weight, as verified by sonication of a lower MW **P1** (66 kDa) and the invariance of the product distribution with time as higher MW polymers are broken down into lower MW fragments (see Supporting Information, Figures S23 and S24, Tables S5 and S6).

This observation is consistent with the diradical model if steric congestion causes a loss of conformational freedom and $k_{rot} < k_{break}$, a shift in trend from the less substituted analogues. Here, rotation is further restricted by the bromine substituents, causing decomposition to the product alkenes with no rotation occuring in the majority of monomers. Comparing this result to unsubstituted *cis*-BCO, we see that any preference for single-inversion is highly suppressed, although the *EZ* product is formed in appreciable quantity (27%). Variations in k_{break} are unlikely to account for the differences. Prior estimates for radical stabilization due to bromine substitution are ~3.5 kcal/mol[54] for a carbon-centered radical, or close to 7 kcal/mol for the diradical implicated here. We calculate that the diacrylate product is stabilized by a similar value of 5 kcal/mol (see Supporting Information, Figure S28), and we therefore infer that the diradical-to-diacrylate bond-breaking step is not significantly impacted by bromination. Figure 7 summarizes product distributions and the proposed mechanistic effects of substitution.

As with most mechanistic considerations, the limiting cases provide a convenient framework for discussion, and we recognize that many subtleties are unresolved. For example, the tetramethylene diradical likely cannot be purely decoupled from C3–C4 scission, as there will be mixing of the non-bonding and bonding orbitals. Likewise, restricted rotation about C1–C4 or C2–C3 might influence the true concertedness of the reaction by slowing C1–C2 homolysis, rather than restricting rotation in the 1,4-diradicaloid intermediate. Nevertheless, these studies show how the outcomes, and presumably the rates, of mechanical BCO activation can be influenced by structural manipulation. Such control might be quite useful, given the potential utility of BCO as a mechanophore in stress-responsive materails.

Conclusion

The bicyclo[4.2.0]octane framework was exploited to develop a family of non-scissile mechanophores. These functionalized cyclobutane bearing units were designed to undergo non-scissile ring opening to afford unsaturated products and high elongations under the application of stress for integration into stress-responsive materials. These mechanophores were incorporated as diol monomers into high molecular weight polyesters via carbodiimide polymerization and subsequently activated to form reactive □, □-unsaturated esters via the application of pulsed ultrasound. Due to the non-scissile nature of the activation, many cycloreversions occur per polymer chain (hundreds) allowing for quantification of reaction progress and determination of products by conventional NMR methods. Small molecule functionalized copolymers as well as network structures were formed via rapid nucleophilic thiol-ene conjugation of mono and difunctional thiols respectively. Reactivity, along with high-elongations (~7 Å per monomer unit) demonstrates an improvement in stress-activated behavior of these mechanophores over that of the *g*DHC systems.[8,22] Moving forward, the

BCO platform will be used to expand and compliment our efforts to develop self-healing materials based on the *g*DHC family of mechanophores. A qualitative assessment of the relative the reactivity of *cis* and *trans*-BCO was made by measuring percent ring opening as a function of sonication time. The stereochemical configurations of product dienes were unambiguously determined for all BCO derivatives and these observations were used to elaborate on a mechanistic description of the mechanochemical [2+2] cycloreversion of cyclobutanes. This model was used to guide our design of substited BCO analogues, allowing us to tune the stereochemical product distributions. Moving forward, we will use molecular dynamics (MD) simulations[38] might help to further address the factors that determine product stereochemistry in this system as well as a more detailed rationalization for the formation of a "pro-*EZ*" conformer. Additionally, efforts are underway to integrate these mechanophores into material platforms that will facilitate bulk activation and the development of mechanochemically stress-responsive materials.

Supplementary Material

Refer to Web version on PubMed Central for supplementary material.

Acknowledgments

This material is based on work supported byby the US Army Research Laboratory and the Army Research Office (grant nos. W911NF-07-1-0409 and W911NF-12-1-0337) and the National Science Foundation (DMR-1122483). Z.S.K. thanks the NIH for a NIGMS Biotechnology Predoctoral Training Grant (T32GM8555). Z.S.K. thanks Jiyong Hong for helpful discussion. We thank Jeff Moore and Matt Kryger for encouraging conversations.

References

1. Piermattei A, Karthikeyan S, Sijbesma RP. Nat Chem. 2009; 1:133–137. [PubMed: 21378826]
2. Wiggins KM, Hudnall TW, Tennyson AG, Bielawski CW. J Mater Chem. 2011; 21:8355–8359.
3. Tennyson AG, Wiggins KM, Bielawski CW. J Am Chem Soc. 2010; 132:16631–16636. [PubMed: 21043506]
4. Wiggins KM, Brantley JN, Bielawski CW. ACS Macro Lett. 2012; 1:623–626.
5. Davis DA, Hamilton A, Yang J, Cremar LD, Van Gough D, Potisek SL, Ong MT, Braun PV, Martinez TJ, White SR, Moore JS, Sottos NR. Nature. 2009; 459:68–72. [PubMed: 19424152]
6. Chen Y, Spiering AJH, Karthikeyan S, Peters GWM, Meijer EW, Sijbesma RP. Nat Chem. 2012; 4:559–562. [PubMed: 22717441]
7. Lenhardt JM, Black AL, Beiermann BA, Steinberg BD, Rahman F, Samborski T, Elsakr J, Moore JS, Sottos NR, Craig SL. J Mater Chem. 2011; 21:8454–8459.
8. Ramirez ALB, Kean ZS, Orlicki JA, Champhekar M, Elsakr SM, Krause WE, Craig SL. Nat Chem. advance online publication. Published Online: Aug 4, 2013. 10.1038/nchem.1720
9. Caruso MM, Davis DA, Shen Q, Odom SA, Sottos NR, White SR, Moore JS. Chem Rev. 2009; 109:5755–5798. [PubMed: 19827748]
10. Akbulatov S, Tian Y, Boulatov R. J Am Chem Soc. 2012; 134:7620–7623. [PubMed: 22540320]
11. Akbulatov S, Tian Y, Kapustin E, Boulatov R. Angew Chem Int Ed. 2013; 52:6992–6995.
12. Kucharski TJ, Huang Z, Yang QZ, Tian YC, Rubin NC, Concepcion CD, Boulatov R. Angew Chem Int Ed. 2009; 48:7040–7043.
13. Yang QZ, Huang Z, Kucharski TJ, Khvostichenko D, Chen J, Boulatov R. Nat Nanotechnol. 2009; 4:302–306. [PubMed: 19421215]
14. Paulusse JMJ, Huijbers JPJ, Sijbesma RP. Chem Eur J. 2006; 12:4928–4934. [PubMed: 16586526]
15. Berkowski KL, Potisek SL, Hickenboth CR, Moore JS. Macromolecules. 2005; 38:8975–8978.
16. Klukovich HM, Kean ZS, Iacono ST, Craig SL. J Am Chem Soc. 2011; 133:17882–17888. [PubMed: 21967190]
17. Chen X, Wudl F, Mal AK, Shen H, Nutt SR. Macromolecules. 2003; 36:1802–1807.

18. Wiggins KM, Syrett JA, Haddleton DM, Bielawski CW. J Am Chem Soc. 2011; 133:7180–7189. [PubMed: 21504196]
19. Black AL, Orlicki JA, Craig SL. J Mater Chem. 2011; 21:8460–8465.
20. Black AL, Lenhardt JM, Craig SL. J Mater Chem. 2011; 21:1655–1663.
21. Klukovich HM, Kouznetsova TB, Kean ZS, Lenhardt JM, Craig SL. Nat Chem. 2013; 5:110–114. [PubMed: 23344431]
22. Wu D, Lenhardt JM, Black AL, Akhremitchev BB, Craig SL. J Am Chem Soc. 2010; 132:15936–15938. [PubMed: 20977189]
23. Kean ZS, Craig SL. Polymer. 2012; 53:1035–1048.
24. Hickenboth CR, Moore JS, White SR, Sottos NR, Baudry J, Wilson SR. Nature. 2007; 446:423–427. [PubMed: 17377579]
25. Wiggins KM, Hudnall TW, Shen QL, Kryger MJ, Moore JS, Bielawski CW. J Am Chem Soc. 2010; 132:3256–3257. [PubMed: 20166664]
26. Klukovich HM, Kean ZS, Ramirez ALB, Lenhardt JM, Lin J, Hu X, Craig SL. J Am Chem Soc. 2012; 134:9577–9580. [PubMed: 22650366]
27. Potisek SL, Davis DA, Sottos NR, White SR, Moore JS. J Am Chem Soc. 2007; 129:13808–13809. [PubMed: 17958363]
28. Hermes M, Boulatov R. J Am Chem Soc. 2011; 133:20044–20047. [PubMed: 22107035]
29. Larsen MB, Boydston AJ. J Am Chem Soc. 2013; 135:8189–8192.
30. Kryger MJ, Munaretto AM, Moore JS. J Am Chem Soc. 2011; 133:18992–18998. [PubMed: 22032443]
31. Kryger MJ, Ong MT, Odom SA, Sottos NR, White SR, Martinez TJ, Moore JS. J Am Chem Soc. 2010; 132:4558–4559. [PubMed: 20232911]
32. Kean ZS, Ramirez Black, AL, Yan Y, Craig SL. J Am Chem Soc. 2012; 134:12939–12942.
33. Moore JS, Stupp SI. Macromolecules. 1990; 23:65–70.
34. Schenck GO, Kuhls J, Krauch CH. Justus Liebigs Ann Chem. 1966; 693:20–43.
35. Beyer MK. J Chem Phys. 2000; 112:7307–7312.
36. Lenhardt JM, Black AL, Craig SL. J Am Chem Soc. 2009; 131:10818–10819. [PubMed: 19603747]
37. Konda SSM, Brantley JN, Bielawski CW, Makarov DE. J Chem Phys. 2011; 135:164103–164108. [PubMed: 22047224]
38. Ong MT, Leiding J, Tao HL, Virshup AM, Martinez TJ. J Am Chem Soc. 2009; 131:6377–6379. [PubMed: 19378993]
39. Boulatov R. Pure Appl Chem. 2010; 83:25–41.
40. Black Ramirez AL, Ogle JW, Schmitt AL, Lenhardt JM, Cashion MP, Mahanthappa MK, Craig SL. ACS Macro Lett. 2011:23–27.
41. Frenkel J. Acta Physicochim URSS. 1944; 19:51–76.
42. Segal GA. J Am Chem Soc. 1974; 96:7892–7898.
43. Hoffmann R, Swaminathan S, Odell BG, Gleiter R. J Am Chem Soc. 1970; 92:7091–7097.
44. Doubleday C, Camp RN, King HF, McIver JW, Mullally D, Page M. J Am Chem Soc. 1984; 106:447–448.
45. Pedersen S, Herek JL, Zewail AH. Science. 1994; 266:1359–1364. [PubMed: 17772843]
46. Baldwin JE, Ford PW. J Am Chem Soc. 1969; 91:7192–7192.
47. Doubleday C. J Am Chem Soc. 1993; 115:11968–11983.
48. Lenhardt JM, Ong MT, Choe R, Evenhuis CR, Martinez TJ, Craig SL. Science. 2010; 329:1057–1060. [PubMed: 20798315]
49. Hoffmann R, Woodward RB. Science. 1970; 167:825–831. [PubMed: 17742608]
50. Genaux CT, Kern F, Walters WD. J Am Chem Soc. 1953; 75:6196–6199.
51. Schaumann E, Ketcham R. Angew Chem Int Ed. 1982; 21:225–247.
52. Robson R, Grubb PW, Barltrop JA. J Chem Soc. 1964:2153–2164.
53. Barltrop JA, Robson R. Tetrahedron Lett. 1963; 4:597–600.

54. Luo, YR. Comprehensive Handbook of Chemical Bond Energies. Taylor & Francis; 2010.

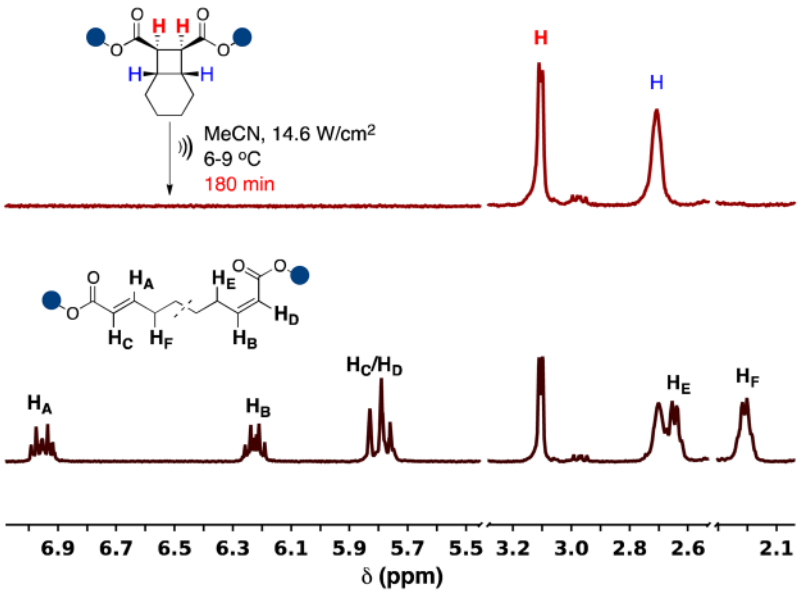

Figure 1.

^{1}H NMR of selected *cis*-BCO peaks before (top) and after (bottom) sonication for 180 minutes shows disappearance of cyclobutane resonances (red and blue) with concurrent appearance of alkene and allyl protons for *E* and *Z* isomers (black).

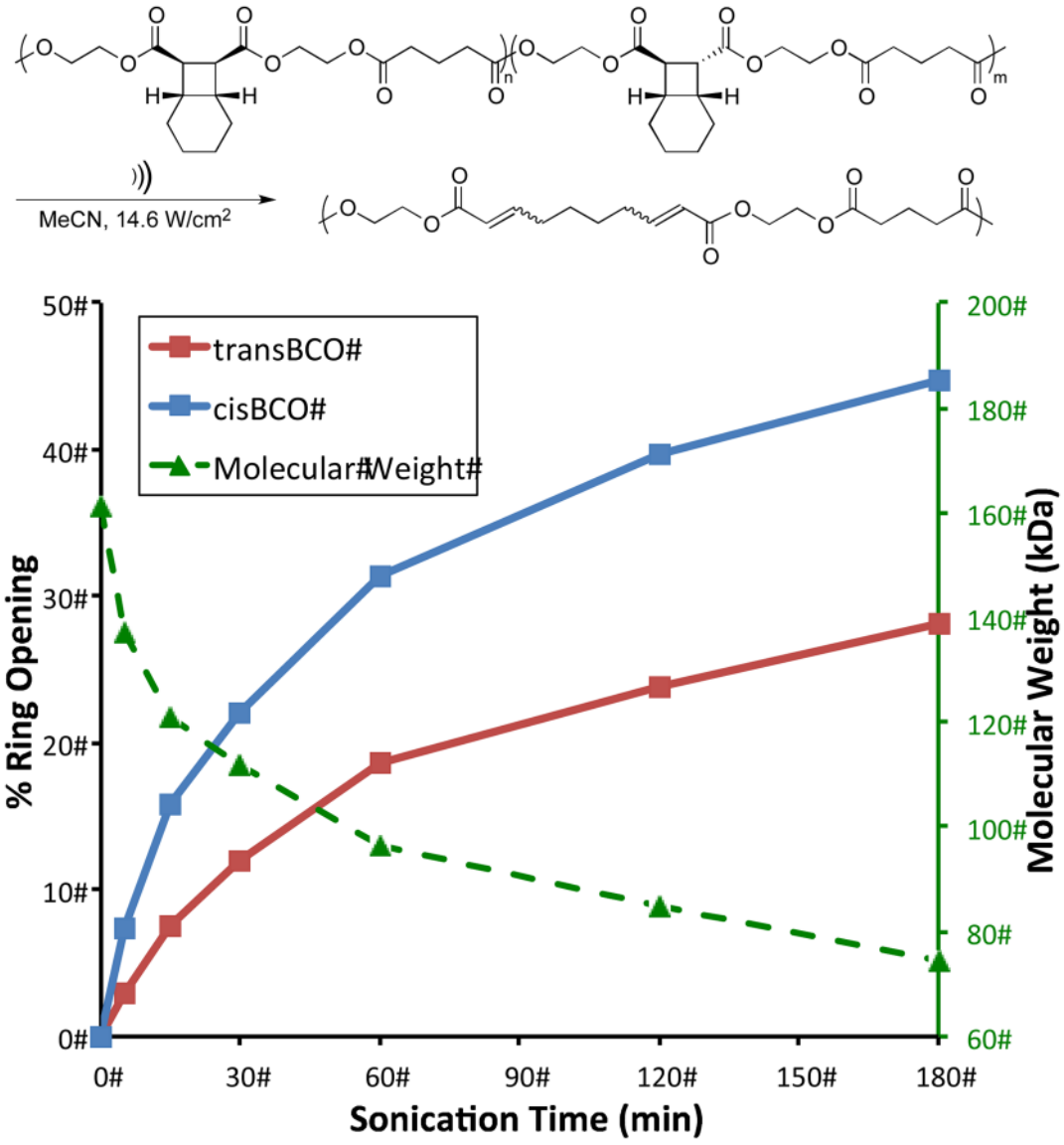

Figure 2.

Sonochemical activation of *cis/trans*-BCO (**P1,2**) copolymer (top) results in different activation profiles for the two isomers as determined by ^{1}H NMR. MW degradation due to non-specific chain scission (green) occurs due to high flow forces experienced in pulsed ultrasound.

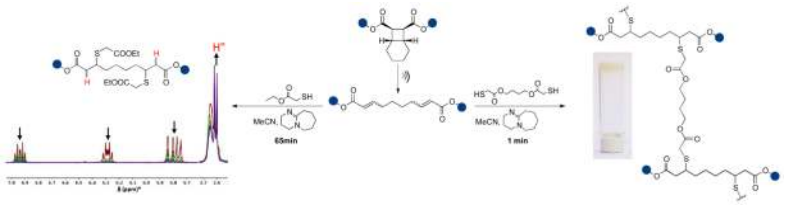

Figure 3.
Stress-enabled reactivity of BCO polymers. Unsaturated esters react via nucleophilic thiol-ene conditions to form functionalized copolymers via reaction with mono-functional thiols (left) and network gels via reaction with bifunctional thiols (right).

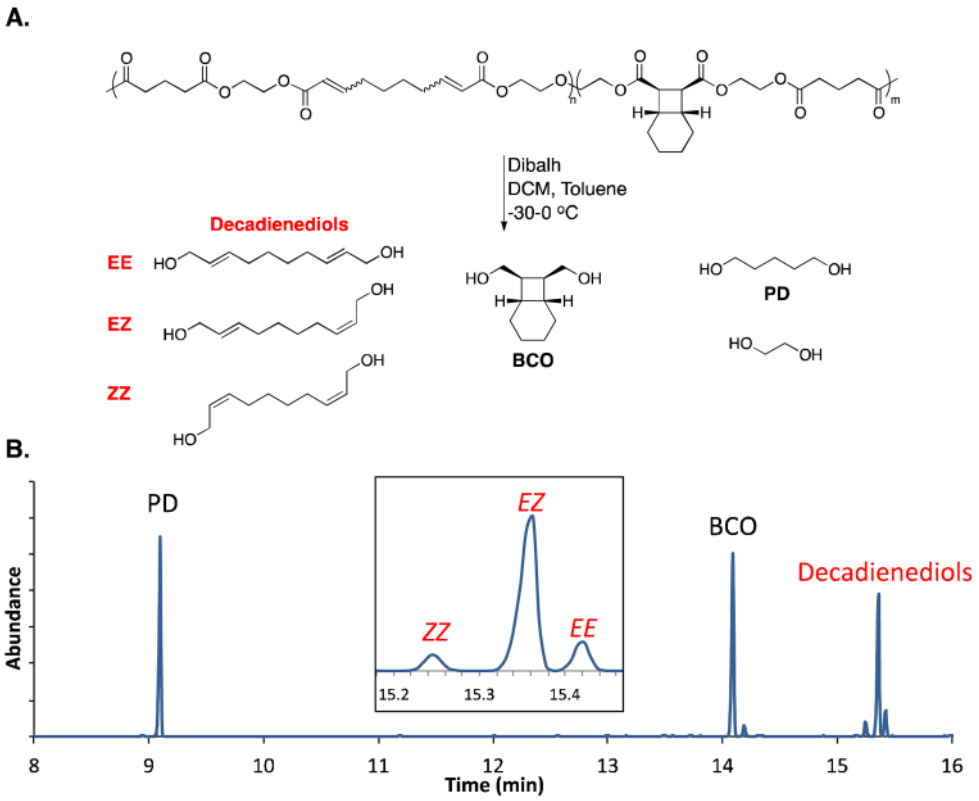

Figure 4.

(A) Reduction of sonicated cis-BCO polymer P1 (52% ring opening) yields constituent small molecule diols. (B) GC analysis of reduction mixture (as TMS-ethers derivatized with BSTFA) shows separation of ZZ, EZ, and EE decadienediol isomers confirmed by comparison with authentic compounds (see Supporting Information)

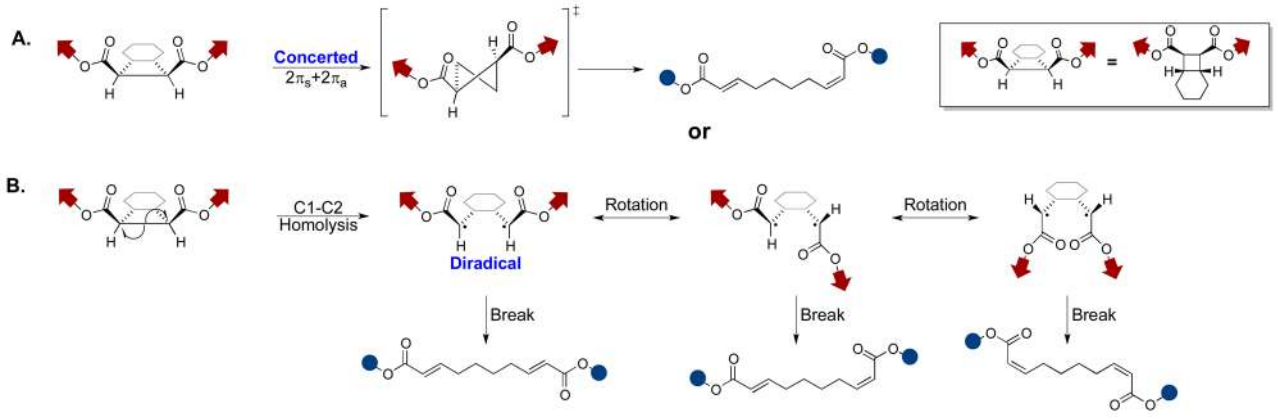

Figure 5.

(A) Hypothetical concerted [2+2]cycloreversion of *cis*-BCO results in *EZ* diene product (B) Diradical intermediate from C1–C2 homolysis allows for conformational freedom and the formation of *EE*, *EZ*, and *ZZ* dienes.

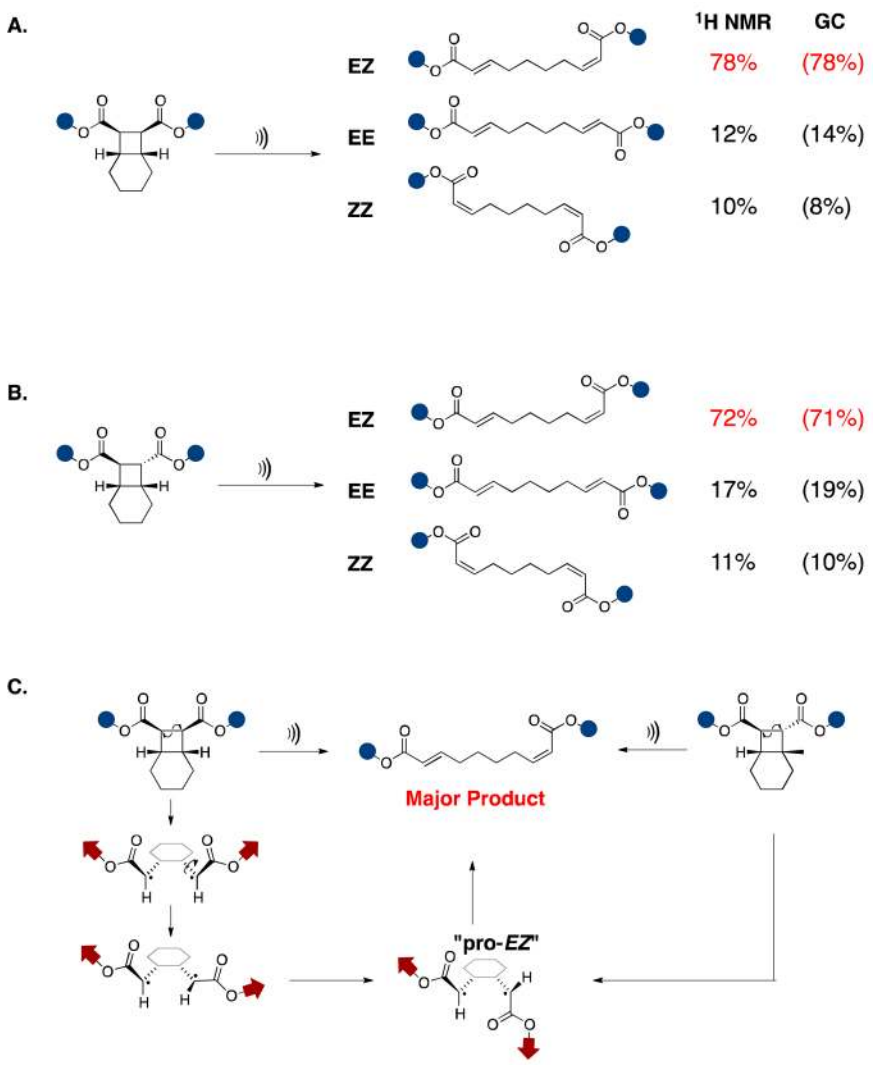

Figure 6.

The *EZ*-diene is the major product of the mechanochemical [2+2] cycloreversion of both *cis*-BCO (A) and *tra*ns-BCO (B). (C) Both isomers are "pulled" into a single "pro-*EZ*" conformer after homolysis resulting in a single major product (red).

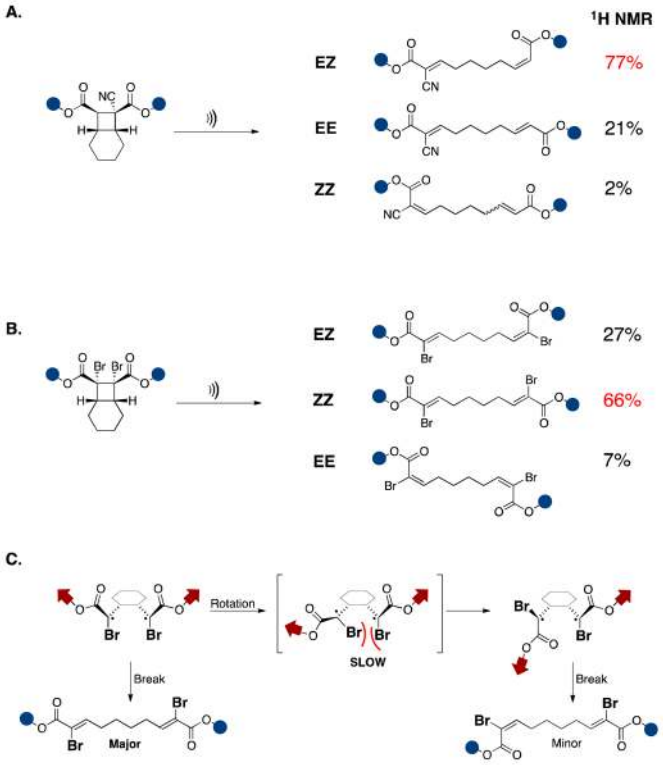

Figure 7.
(A) Product distribution of mechanochemical activation of *cis*-CN-BCO polymer **P3**. (B) Product distribution of mechanochemical activation of *cis*-Br_2-BCO polymer **P4**. (C) Increased substitution hinders diradical rotation resulting in increased retention of stereochemistry. Major products shown in red.

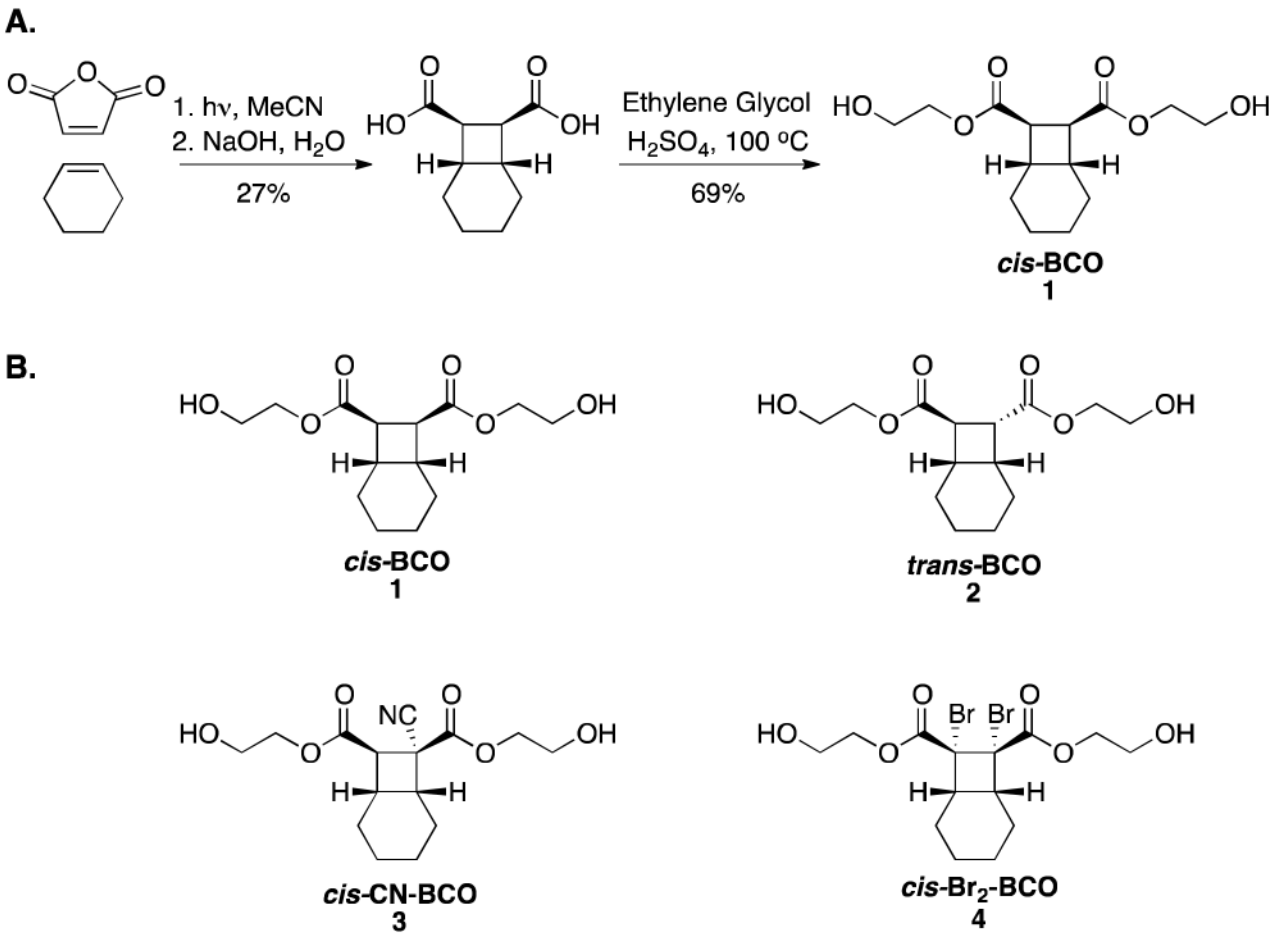

Scheme 1.

(A) Representative synthesis of BCO diol monomer (B) Structures of BCO diol analogues

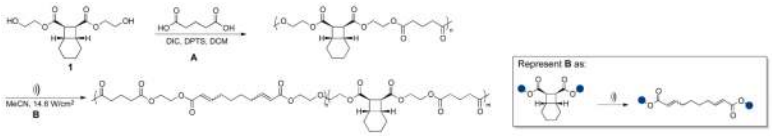

Scheme 2.

Carbodiimide polyesterification of BCO-diol (1) and mechanochemical activation by pulsed ultrasound. Blue dots symbolize the polymer structure surrounding BCOs in unactivated polymers and alkenes in activated copolymers (inset).

Table 1

Summary of Polymers Synthesized[a]

Polymer Name	BCO Diol	M_n (kDa)	PDI
P1 (*cis*-BCO)	1	179	1.43
P2 (*trans*-BCO)	2	155	1.34
P1,2 (*cis/trans*-BCO)	1 & 2	161	1.32
P3 (*cis*-CN-BCO)	3	133	1.28
P4 (*cis*-Br_2-BCO)	4	51.0	1.35
PC (control)	1 & 2	13.3	1.28

[a]Polymers were synthesized according to the method outlined in Scheme 2 from their respective diol monomers shown in Scheme 1. MWs (M_n) and PDI were determined by GPC-MALS (see Supporting Information).